Active Ti Species in $TiCl_3$-Doped $NaAlH_4$. Mechanism for Catalyst Deactivation

Cornelis P. Baldé,[†] Hans A. Stil,[‡] Ad M. J. van der Eerden,[†] Krijn P. de Jong,[†] and Johannes H. Bitter*,[†]

Inorganic Chemistry and Catalysis, Department of Chemistry, Faculty of Sciences, Universiteit Utrecht, Sorbonnelaan 16, 3584 CA Utrecht, The Netherlands, and Shell Research and Technology Centre, Badhuisweg 3, 1031 CM Amsterdam, The Netherlands

Received: July 26, 2006; In Final Form: October 9, 2006

The nature of the active Ti species in $TiCl_3$-doped $NaAlH_4$, a promising hydrogen storage material, was studied as a function of the desorption temperature with Ti K-edge extended X-ray absorption fine structure (EXAFS) spectroscopy, Ti K-edge X-ray absorption near-edge structure (XANES) spectroscopy, and X-ray diffraction (XRD). In the freshly prepared sample, Ti was amorphous and surrounded by 4.8 Al atoms divided between two shells at 2.71 and 2.89 Å. In the next shell, 1.9 Ti atoms were detected at 3.52 Å. It was concluded that 30% of Ti was incorporated into the surface of Al crystallites and 70% of Ti occupied interstitials in the $NaAlH_4$ lattice, possibly forming trimeric, triangular Ti entities. After hydrogen desorption at 125 °C, $NaAlH_4$ decomposed and the Ti−Al coordination number increased from 4.8 to 8.5. We propose that all Ti is incorporated into the surface layer of the formed Al. After the material was heated to 225 °C, the local structure of Ti, as inferred from EXAFS and XANES spectroscopy, was identical to the local structure of a $TiAl_3$ alloy. However, the formed alloy was amorphous and was only detected in XRD by an increase of the background intensity around the Al diffraction. These so-called "$TiAl_3$ clusters" agglomerated in the heat treatment to 475 °C, forming crystalline $TiAl_3$. Earlier work has shown that increasing the desorption temperature of $NaAlH_4$ lowers the absorption rate and capacity of hydrogen in the next step. Thus, by comparing our results with absorption properties published in the literature on similar samples, we could rank the activity of the Ti for hydrogen absorption as Ti in the Al surface > $TiAl_3$ cluster > crystalline $TiAl_3$, therewith indicating that Ti incorporated into the surface of Al is the most active for the absorption of hydrogen.

Introduction

In the future new sustainable energy sources and carriers will be needed. Hydrogen is attractive as an energy carrier since it has a high energy to mass ratio and produces water as its only waste product.[1,2] Conventional storage technologies, such as gas compression or cryogenic liquid, have limitations related to safety aspects and low volumetric hydrogen densities.[2,3] Storing hydrogen by chemical bonding or physisorption may circumvent these problems. Several storage media are considered, e.g., nanosized magnesium hydride,[4] physisorption on carbon,[5,6] and sodium alanate ($NaAlH_4$).[2,7] Sodium alanate is promising since its thermodynamic properties enable reversible storage of hydrogen at low temperatures for on-board applications. Hydrogen is desorbed in three steps (eqs 1−3) with respective equilibrium temperatures of 30, 110, and >400 °C at 1 bar of hydrogen pressure. The first two desorption temperatures are compatible with on-board storage and deliver a total of 5.6 wt % hydrogen storage capacity.

$$NaAlH_4 \leftrightarrow {}^1/_3Na_3AlH_6 + {}^2/_3Al + H_2 \quad (1)$$

$$Na_3AlH_6 \leftrightarrow 3NaH + Al + 1{}^1/_2H_2 \quad (2)$$

$$NaH \leftrightarrow Na + {}^1/_2H_2 \quad (3)$$

The main hurdle to overcome for applying $NaAlH_4$ as a hydrogen storage material is the slow kinetics for hydrogen desorption and absorption. These unfavorable desorption and absorption rates can be improved by reducing the particle size of the $NaAlH_4$ to the nanometer range[8] or by adding a catalyst, for example, $TiCl_3$ or titanium butoxide, to the alanate.[7,9,10] Generally, the most active catalyst is prepared by ball milling $NaAlH_4$ with the $TiCl_3$,[10] resulting in a reaction to form NaCl, Al, and a reduced Ti entity as shown in reaction 4.[11]

$$TiCl_3 + 3NaAlH_4 \rightarrow \text{"Ti"} + 3Al + 3NaCl + 6H_2 \quad (4)$$

The correlation among the catalytic role, structure, and location of the Ti for (de)hydriding catalysis is not fully understood, although it has been the subject of many investigations in the past years.[12−28] A H_2/D_2 scrambling study performed by Schüth et al. points out that the Ti after doping dissociates hydrogen at room temperature, suggesting that one of the roles of the Ti catalyst might be to split hydrogen.[12] Alternatively, it is suggested that Ti facilitates migration of H via interstitials[13] or facilitates migration of metal atoms in the form of AlH_3 units.[14,15] It has also been reported that the Ti does not solely change the kinetics, but also alters the thermodynamics of the Ti-doped $NaAlH_4$ system.[16] The structure and catalytic cycle of the active Ti species for these functions have not been identified in these studies.

A variety of Ti species have been proposed or calculated to be catalytically active. Some authors claim that Ti alloys with Al as an amorphous species upon doping $TiCl_3$ with $NaAlH_4$,[9,17−19] while others observed the formation of metallic Ti clusters.[20] Jensen et al. claim on the basis of an IR spectroscopy study that Ti is located in the vicinity of the AlH_4^- unit and influences the Al−H asymmetric stretching frequency.[21] Some DFT

* To whom correspondence should be addressed. Tel.: +31-30-2536778; Fax: +31-30-2511027; E-mail: j.h.bitter@chem.uu.nl.
† Universiteit Utrecht.
‡ Shell Research and Technology Centre.

10.1021/jp064765q CCC: $37.00
Published on Web 01/25/2007

calculations show that Ti preferably substitutes Na sites[14,22,23] or occupies interstitial positions in the $NaAlH_4$ lattice.[24] Contrarily, Løvvik and Opalka claim that Ti primarily moves to interfaces between Al and $NaAlH_4$, grain boundaries, or to defects in the $NaAlH_4$ particles.[25] Alternatively, it is also reported that Ti on an Al surface might be the active Ti entity.[26−28]

Geerlings et al. showed that the rate of hydrogen reloading decreases with increasing temperature of the preceding hydrogen desorption step.[9] Thus, by comparing the Ti species in the samples after different desorption temperatures, more information might be obtained on the nature of the (in)active Ti species. Ti was mostly present as an amorphous phase, making analysis challenging with a single technique. Therefore, the structure of Ti-containing $NaAlH_4$ was characterized using extended X-ray absorption fine structure (EXAFS) spectroscopy, X-ray absorption near-edge structure (XANES) spectroscopy, and X-ray diffraction (XRD) in this paper. A structure−activity relationship is proposed on the basis of the derived structure of Ti.

Experimental Section

Sample Preparations. All sample preparations were performed under a nitrogen or argon atmosphere in a glovebox equipped with a circulation purifier. Chemical operations were conducted using Schlenk techniques. To prevent hydrogen desorption and possible changes in the samples, transportation and storage were performed at 5 °C or below under an inert atmosphere. Commercially available $NaAlH_4$ (tech. 90%, Sigma-Aldrich) was purified and ball-milled with 10 mol % $TiCl_3$ by the authors of ref 9 as described before. This sample is referred to as "SAH-start". This sample was split into three parts; the respective parts were heated in Ar to 125, 225, and 475 °C with a ramp of 5 °C/min. The samples were kept at the final temperature until no detectable hydrogen desorption was recorded by volumetric analysis. The samples are called "SAH-125", "SAH-225", and "SAH-475", respectively. The XRD diffraction patterns, curves of the first desorption step, and hydrogen storage capacities are identical to those reported in a previous paper.[9]

EXAFS Spectroscopy. X-ray absorption spectroscopy was performed on the Ti K-edge at station E4 of the DESY synchrotron (Hamburg, Germany). The storage ring was operated at 4.4 GeV with a mean current of 120 mA, using a Si(111) double-crystal monochromator that was detuned to 80% to suppress higher harmonics. Measurements were performed at 77 K in flowing He to exclude thermal decomposition of the sample. The samples (11 mg of Ti-doped $NaAlH_4$ or 6 mg of $TiAl_3$) had a total absorption of 2.55 and were homogeneously diluted with 50 mg of BN, pressed into a pellet, mounted to the cell, and transferred to the beamline in a closed cell.

Extraction of the EXAFS data from the measured absorption data was performed with the XDAP program.[29] Three scans were averaged, and the pre-edge background was approximated by a Victoreen function before subtraction.[30] The position of the edge energy was determined at the maximum of the first derivative of the spectrum and was calibrated using a Ti foil as a reference in each scan. The spectrum was background corrected by employing a cubic spline routine.[31] Normalization was performed by dividing the absorption spectrum by the height of the background 50 eV from the edge.

The Ti−Al backscattering amplitude and phase shift were calculated using the FEFF 8.2 code[32] and calibrated using an experimentally measured spectrum of $TiAl_3$ at 77 K. EXAFS spectroscopy of a Ti foil at room temperature was used to calibrate the Ti−Ti calculated reference. The FEFF input parameters for the references are listed in Table 1.

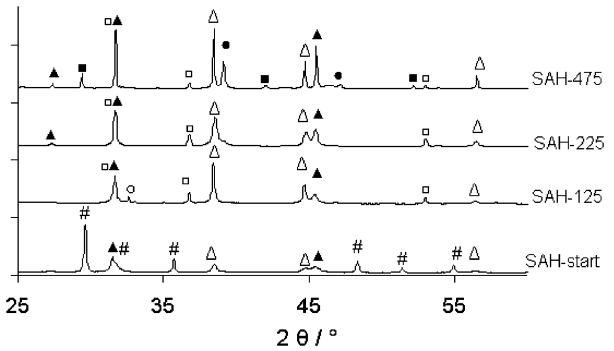

Figure 1. XRD patterns of SAH-start, SAH-125, SAH-225, and SAH-475: (#) $NaAlH_4$, (△) Al, (▲) NaCl, (□) NaH, (○) Na_3AlH_6, (■) Na, (●) $TiAl_3$.

TABLE 1: Input Parameters To Create FEFF-Calculated Ti−Al and Ti−Ti References

	ref compd	S_0^2	σ^2/ 10^3 Å^{-2}	V_r/ eV	V_i/ eV	potential
Ti−Al	$TiAl_3$	0.72	1.5	11.3	1.0	Hedin−Lunqvist
Ti−Ti	hcp Ti foil	0.60	0	8.6	1.0	Hedin−Lunqvist

Experimental data were fitted in k^2 using the difference file technique in R space[33] at $3 < k$ (Å^{-1}) < 10 or $3 < k$ (Å^{-1}) < 12 depending on the quality of the data. The quality of the fit was checked by applying k^1, k^2, and k^3 weightings, ensuring that the correct coordination number and Debye−Waller factor ($\Delta\sigma^2$) were fitted.[33]

Errors in the numerical values obtained by EXAFS data analysis are estimated to be ±10% in the coordination number (N), ±1% in the distance (R), ±5% in the Debye−Waller factor ($\Delta\sigma^2$), and ±10% for inner potential correction.[34]

XANES Spectroscopy. XANES spectra were recorded from 4950 to 5050 eV with a step size of 0.3 eV. The position of the edge was set at the maximum of the first derivative (inflection point) of the first rising edge. The spectra were normalized to 5020 eV.

XRD. X-ray diffraction patterns were recorded on a Panalytical X'pert Pro system using Cu Kα radiation. Samples were transferred to the instrument in airtight sample holders. The data were collected in the range $2\theta = 15-85°$ with a step size of 0.033°. Qualitative analysis was done by comparison with entries from the ICDD PDF22000 database.

Results

To confirm that our samples were identical to those described in ref 9, an XRD study was carried out. Figure 1 shows the XRD pattern of the materials after they were heated to different temperatures. Different possible phases were identified ($NaAlH_4$, Na_3AlH_6, Al, Na, NaCl, NaH, $TiAl_3$) and are indicated in the figure. In SAH-start, $NaAlH_4$, NaCl, and Al were detected. The latter two phases were expected on the basis of the doping reaction (eq 4). After the material was heated to 125 °C, the diffraction lines representing $NaAlH_4$ disappeared (Figure 1, SAH-125), while those of NaCl, NaH, Al, and Na_3AlH_6 were present. This is in line with the desorption reactions shown in eqs 1 and 2. In SAH-225 only diffractions from NaH, Al, and NaCl were present, indicating that all hydrogen relating to reactions 1 and 2 was desorbed. After the hydrogen was desorbed at 475 °C, Al, Na, NaCl, NaH, and $TiAl_3$ were observed. The presence of Na indicates that at this high temperature NaH was partly dehydrogenated.

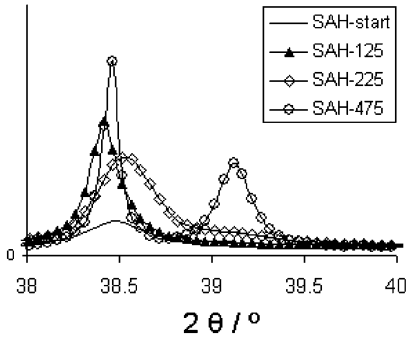

Figure 2. XRD Al diffraction lines for SAH-start, SAH-125, SAH-225, and SAH-475.

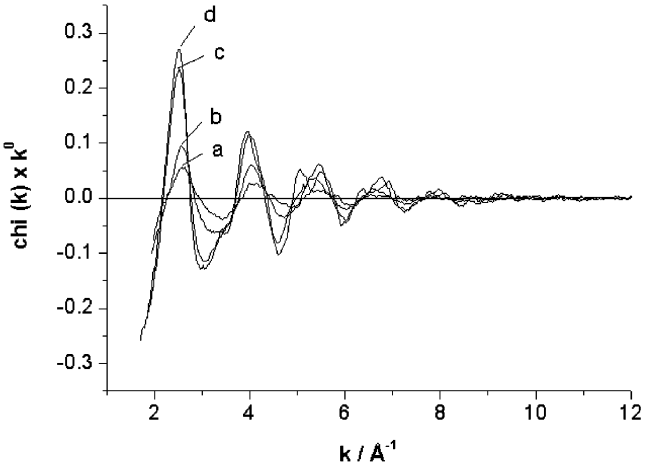

Figure 3. k^0-weighted background-subtracted $\chi(k)$ of (a) SAH-start, (b) SAH-125, (c) SAH-225, and (d) SAH-475.

Titanium was only detectable as a crystalline phase in SAH-475. Amorphous Ti species have been claimed to be indirectly visible in XRD via the Al diffraction peaks.[9,18,19] Therefore, the diffraction peak of Al metal is shown in detail in Figure 2. An increase of the background was observed for $2\theta = 38.7-39.5°$ after the sample was heated to 225 °C (SAH-225), indicating the presence of an amorphous phase. In contrast, the materials after ball milling (SAH-start) and after desorption at 125 °C (SAH-125) and 475 °C (SAH-475) did not show this increase in background intensity.

To get more insight regarding the structure of the amorphous Ti, the local structure of Ti was investigated with EXAFS spectroscopy. The background-subtracted EXAFS data, $\chi(k)$, of SAH-Start, SAH-125, SAH-225, and SAH-475 are shown in Figure 3. It can be seen that the quality of the data was good. The k^1-weighted Fourier-transformed data are shown in Figure 4 (top panel, magnitude; lower panel, imaginary part). From the changes in the magnitude and the positions of the nodes in the imaginary part it can be concluded that the local environment around Ti changed significantly with the desorption temperature.

The fitted and raw data for SAH-start are shown in Figure 5. Table 2 shows the fit parameters and k^2 variances of SAH-start, SAH-125, SAH-225, SAH-475, and the reference $TiAl_3$. The k^2 variances were low and in the same range, indicating that the fits were of comparable quality. For all measured samples, Al always surrounded Ti in the first two coordination shells. In the third shell, Ti was found at a longer distance. The fit for $TiAl_3$ exactly matches the known crystallographic data[35] of this sample; i.e., Al is distributed in two shells located at 2.73 and 2.88 Å with, respectively, four and eight Al atoms (please note that the first Ti−Al shell was used to calibrate the Ti−Al reference), and four Ti atoms were detected at 3.89 Å.

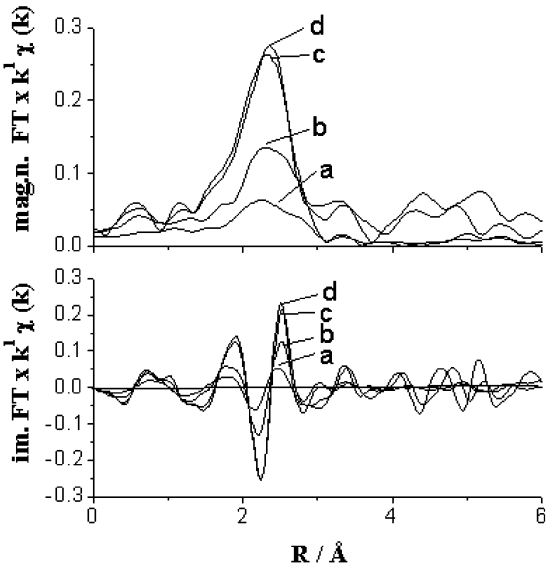

Figure 4. Magnitude and imaginary part of Fourier-transformed $\chi(k)$: (a) SAH-start, (b) SAH-125, (c) SAH-225, (d) SAH-475 (k^1; $\Delta k = 3-12$ Å^{-1}).

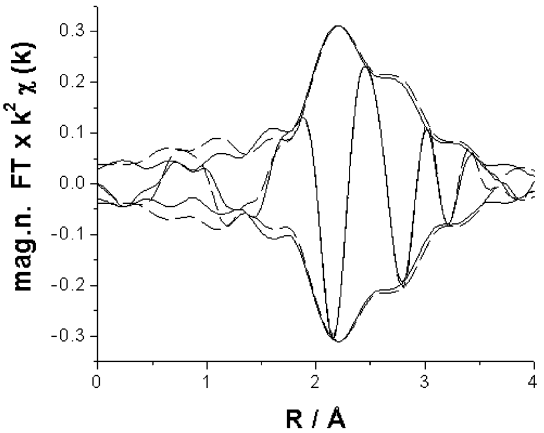

Figure 5. k^2-weighted phase-uncorrected Fourier transform of SAH-start (solid line) and the fit ($\Delta k = 3-12$ Å^{-1}, $\Delta R = 1.2-3.5$ Å) (dashed line).

TABLE 2: EXAFS Fits of SAH-start, SAH-125, SAH-225, and SAH-475[a]

name	shell	atom	N	$\Delta\sigma^2$/ 10^3 Å^{-2}	R/ Å	E_o/ eV	k^2 variance imag	k^2 variance abs
SAH-start	1	Ti−Al	2.3	0.04	2.71	−0.96	0.63	0.40
	2	Ti−Al	2.5	0.18	2.89	0.96		
	3	Ti−Ti	1.9	0.81	3.52	1.93		
SAH-125	1	Ti−Al	3.9	0.20	2.76	−1.19	0.90	0.44
	2	Ti−Al	4.6	0.20	2.92	0.23		
	3	Ti−Ti	1.3	2.70	3.49	4.30		
SAH-225	1	Ti−Al	4.6	0.10	2.73	1.53	0.36	0.23
	2	Ti−Al	7.8	0.82	2.84	4.97		
	3	Ti−Ti	3.8	6.36	3.90	4.31		
SAH-475	1	Ti−Al	4.2	0.36	2.75	3.11	0.43	0.27
	2	Ti−Al	8.3	1.95	2.89	3.70		
	3	Ti−Ti	3.8	3.25	3.84	5.44		
$TiAl_3$	1	Ti−Al	4.0	0.00	2.73	−0.47	2.13	1.00
	2	Ti−Al	8.0	1.53	2.88	4.12		
	3	Ti−Ti	4.0	4.83	3.89	1.85		

[a] The number of independent parameters (Nyquist theorem)[38] was 17, and the data were fitted with 12 parameters.

Taking into account the ±10% error of the coordination number and the ±1% error in distance,[34] the local environment of Ti in SAH-475 and SAH-225 was identical to that of Ti in the reference sample $TiAl_3$.

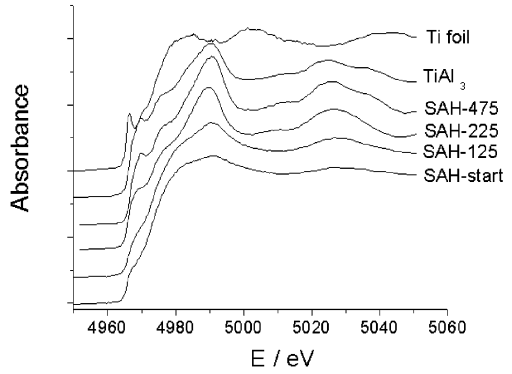

Figure 6. XANES spectra of SAH-start, SAH-125, SAH-225, SAH-475, $TiAl_3$, and Ti foil.

TABLE 3: Positions of Ti Edges in SAH-start, SAH-125, SAH-225, SAH-475, and $TiAl_3$

	edge position (eV)		edge position (eV)
SAH-start	4965.7	SAH-475	4966.7
SAH-125	4965.7	$TiAl_3$	4966.7
SAH-225	4966.1	Ti foil	4965.5

In contrast, the local structure of SAH-125 comprised in total 8.5 Al atoms in its first and second Al shells, 3.9 Al at 2.76 Å and 4.6 Al atoms at 2.92 Å. Thus, the total coordination number of the Al sphere (8.5) was significantly lower than in $TiAl_3$, in which 12 Al atoms surround Ti. In addition, the Ti−Ti distance in SAH-125 was 3.49 Å, which is significantly shorter than the Ti−Ti distance of 3.89 Å in $TiAl_3$.

For the sample prior to hydrogen desorption (SAH-start), 2.3 Al atoms at 2.71 Å and 2.5 Al atoms at 2.89 Å surrounded Ti in the first coordination sphere. The next sphere contained 1.9 Ti atoms at 3.49 Å, which was approximately the same as in SAH-125.

XANES spectra of SAH-start, SAH-125, SAH-225, SAH-475, and $TiAl_3$ are shown in Figure 6. It is observed that the XANES spectra of $TiAl_3$, SAH-475, and SAH-225 are identical. In contrast, the XANES spectra of SAH-start and SAH-125 show similar characteristics and differed from that of $TiAl_3$. The positions of the absorption edge for the measured samples are listed in Table 3 and were between those of Ti-foil and $TiAl_3$.

Discussion

Structure of Ti as a Function of the Desorption Temperature. The position of the Ti absorption edge is affected by the oxidation state of Ti. When the formal oxidation state of Ti was zero, for instance, in Ti metal and $TiAl_3$, the edge positions were, respectively, at 4965.5 and 4966.7 eV (Table 3). After doping (SAH-start), the position of the Ti edge was at 4965.7 eV, which was between that of $TiAl_3$ and Ti (Figure 6 and Table 3). Thus, Ti had a (close to) zero oxidation state after doping, which is in agreement with the doping reaction 4. Linear analysis methods did not indicate substantial (>10%) oxidation of the Ti. The XANES features of SAH-start and $TiAl_3$ were different, indicating a different geometry and/or electronic state for Ti in SAH-start compared to $TiAl_3$. The structural differences were further revealed by EXAFS spectroscopy. In SAH-start (Table 2) Ti was surrounded by on average 2.3 and 2.5 Al atoms at 2.71 and 2.89 Å in the two closest coordination shells. This is significantly lower than the Ti−Al coordination number in $TiAl_3$, which was 4 in the first shell and 8 in the second (Table 2 and ref 35). The structure of the subcoordinated Ti species in SAH-start will be discussed now.

SCHEME 1: (a) Structure of $NaAlH_4$(110), (b) Interstitial Ti in $NaAlH_4$, and (c) Two Ti Atoms Added to Adjacent Interstitial Positions, Forming a Trimeric Triangular Entity[a]

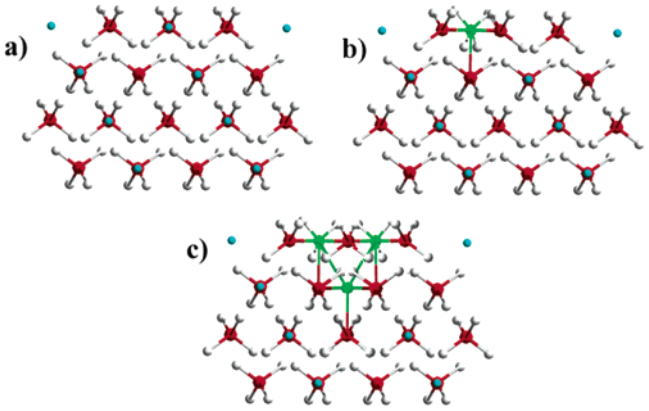

[a] Key: hydrogen, white; aluminum, red; sodium, blue; titanium, green.

XRD (Figure 1) shows that in SAH-start $NaAlH_4$, Al, and NaCl are present as crystalline materials. Since Ti is inert toward NaCl, Ti must have interacted with either Al or $NaAlH_4$ or formed a separate Ti phase. Since fitting of one or both of the first shells with Ti−Ti scattering (not shown) did not result in satisfactory fits, it was concluded that no measurable concentration of Ti clusters was formed during doping. Thus, Ti must have interacted with Al or $NaAlH_4$. When Ti interacts with $NaAlH_4$, it has been reported that Ti can substitute for Na[14,22,23] or occupies an interstitial position among three AlH_4^- units.[24] In the case that Ti substitutes for Na, the resulting Al−Ti distance would be approximately 3.5 Å, which is a distance that was not observed for Ti−Al scattering in our EXAFS analysis (Table 2). Therefore, we conclude that the Ti did not substitute for Na to a measurable extent. When Ti is interstitial in the $NaAlH_4$ lattice, the DFT-calculated Ti−Al distance is approximately 2.6 Å.[24] This distance is, within the error limits of the calculation, similar to that found in our EXAFS analysis, and interstitial Ti in $NaAlH_4$ is a reasonable suggestion for a phase present in SAH-start. Three aluminum atoms surrounded the Ti in this species; thus, assuming that all Ti is interstitial, the Ti−Al coordination number should be 3. Since the observed Ti−Al coordination number is 4.8 (Table 2), Ti must also be present in another phase as well with a higher coordination number. Two other locations for the Ti can be envisioned, i.e., on/in the Al phase or as a Ti−Al alloy. XRD (Figures 1 and 2) did not indicate that Ti formed a crystalline phase with Al; thus, bulk alloying did not occur to a large extent. Chaudhuri et al. have calculated that a Ti capped by H atoms and incorporated into the Al surface is stable.[26] When Ti is incorporated into the surface of Al metal, the Ti−Al distance is expected to be in the range of 2.7−2.9 Å.[26] These values agree with those found in our EXAFS analysis (Table 2); therefore, we propose that part of the Ti is located at the Al surface. When the Ti is incorporated into a surface, the close-packed fcc structure of Al metal is 9 Al atoms around the Ti. On the basis of the use of fractional coordination numbers, it can be calculated that 30% of the Ti resided in the Al surface with a coordination number of 9 and 70% was located in an interstitial place in $NaAlH_4$ with a coordination number of 3 ($(0.7 \times 3) + (0.3 \times 9) = 4.8$).

The structure of the interstitial Ti during doping is schematically represented in Scheme 1. Scheme 1a shows the $NaAlH_4$ lattice; after ball milling $TiCl_3$ reacts with $NaAlH_4$, forming

SCHEME 2: (a) View Parallel to the (111) Al Surface (Red) with Ti (Green) Incorporated into the Surface Having a Distorted Local Structure[a] and (b) View Parallel to the (111) Al Surface of Ti That Migrated from the Surface into the Bulk, Forming a $TiAl_3$ Cluster[b]

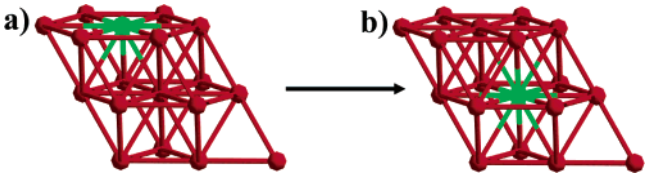

[a] The Ti in SAH-125 predominantly displayed this structure. [b]This resembles the composition of SAH-225.

NaCl and Al metal (eq 4). The formed NaCl and Al are excluded from the picture to clarify the Ti occupying an interstitial site in the $NaAlH_4$ lattice (Scheme 1b). EXAFS analysis of SAH-start (Table 2) also shows that a Ti−Ti distance at 3.52 Å was present. This Ti−Ti distance does not appear in Ti metal, any titanium hydride phase, or Ti−Al alloy. In $TiCl_3$, the Ti−Ti distance is 3.53 Å.[36] Thus, if the $TiCl_3$ is present, Ti−Cl bonds at 2.46 Å must be detected too. Attempts to fit this distance with an FEFF 8.2 calculated Ti−Cl reference were not successful. Moreover, an XPS depth profiling study indicates that the $TiCl_3$ is completely reduced after 30 min of ball milling,[37] whereas the samples investigated in the current study were milled for 1 h. Thus, $TiCl_3$ was most likely not present in SAH-start.

The distance between two interstitial spaces in an unperturbed $NaAlH_4$ lattice is 3.7 Å. Thus, we hypothesize that the Ti−Ti distance found in EXAFS analysis originated from Ti atoms occupying adjacent interstitial spaces in the $NaAlH_4$ lattice. The observed coordination number of Ti−Ti is 1.9; thus, a trimeric triangular Ti species occupying three neighboring interstitials is proposed to explain these observations (Scheme 1c). The deviation between interstitial distances in $NaAlH_4$ (3.7 Å) and the interstitial Ti−Ti distance (3.5 Å) found in EXAFS analysis is possibly due to the fact that the presence of Ti atoms in adjacent interstitial spaces distorts the local structure.

The evolution of the Ti species was further investigated after hydrogen desorption at different temperatures. After desorption at 125 °C, the XRD pattern of SAH-125 revealed that NaH, Al, Na_3AlH_6, and NaCl were present (Figure 1), indicating that $NaAlH_4$ was completely converted. In the starting material (SAH-start), 70% of Ti was present in $NaAlH_4$ interstitials; thus, the local structure of Ti must have been changed during desorption since $NaAlH_4$ was absent in SAH-125. In the EXAFS fits (Table 2) the total coordination number of the first two Ti−Al shells increased from 4.8 to 8.5 (SAH-start to SAH-125). The Ti−Al coordination of 8.5 in SAH-125 is very close to the coordination number when Ti is substituted in the Al(111) surface, in which Ti has 9 Al atoms in its coordination sphere (see Scheme 2a). The aluminum was present in two shells around Ti, at distances of 2.76 and 2.92 Å. In an ideal fcc lattice, the Ti is only surrounded by a single Ti−Al shell. This indicates that the local structure was probably distorted with respect to the ideal fcc geometry. Thus, we conclude that the majority of the Ti was present at the Al surface having a distorted local structure after desorption at 125 °C, which is schematically shown in Scheme 2a.

The local structure of Ti in SAH-125 revealed a Ti at 3.49 Å (Table 2), whereas a Ti atom at ∼3.8 Å would be expected on the basis of the structure of $TiAl_3$.[35] This led us to the speculation that a distorted surface Ti−Al species was formed, leading to a Ti atom in a contracted third shell.

When the hydrogen was desorbed at 225 °C, it was found that the local structures of SAH-225 and $TiAl_3$ were the same within the sensitivity of EXAFS spectroscopy (Table 2). This was also confirmed by XANES spectroscopy (Figure 6), which showed a high similarity of the spectra SAH-225 and $TiAl_3$. The diffraction line of crystalline $TiAl_3$ was not detected in XRD (Figure 1), but the magnification of the Al diffraction (Figure 2) shows that the background was increased from $2\theta = 38.7°$ to $2\theta = 39.5°$. This indicates that an amorphous Ti−Al alloy is formed and has been explained by the presence of an intermetallic $TiAl_x$ species by Geerlings et al.[9] Thus, the local structure of Ti was identical to the local structure of $TiAl_3$, and we suggest that $TiAl_3$ clusters were formed at 225 °C. Thus, between 125 and 225 °C, Ti had migrated from the Al surface to the bulk of aluminum, which is visualized in Scheme 2.

When the desorption temperature was 475 °C, the local structure around Ti did not change significantly compared to that after desorption at 225 °C, as seen in Table 2. However, XRD showed that a crystalline $TiAl_3$ alloy was formed at this temperature (Figure 2). Thus, the $TiAl_3$ clusters in SAH-225 had agglomerated to a crystalline $TiAl_3$ phase on going from 225 to 475 °C.

Catalyst Deactivation. The XRD study reproduced the results of Geerlings et al. (ref 9), indicating that the current samples are identical to the ones used before. Their research indicated that the hydriding activity decreased with an increasing desorption temperature in the preceding step. The activity of the Ti catalyst increased thus in the order SAH-125 > SAH-225 > SAH-475. In the most active sample (SAH-125), it was concluded in the preceding chapter that the majority of Ti was incorporated into the Al surface having a distorted local structure. Thus, we propose that this is the most active form of Ti in the Ti-doped $NaAlH_4$. The Ti catalyst deactivated as the Ti migrated into the Al metal, which occurred between 125 and 225 °C (Scheme 2). The deactivation continued when the $TiAl_3$ clusters agglomerated, forming crystalline $TiAl_3$, which occurred between 225 and 475 °C. This decreases the dispersion of the Ti catalyst, probably resulting in an impaired accessibility of the Ti catalyst. Thus, the activity of the Ti catalyst can be summarized in the following sequence:

Ti in the Al surface > $TiAl_3$ cluster > crystalline $TiAl_3$

Conclusions

In $NaAlH_4$ ball milled with $TiCl_3$, the majority (∼70%) of Ti occupied interstitial spaces in the $NaAlH_4$ lattice. The remaining Ti was present at the surface of Al. After desorption at 125 °C the majority of Ti was present at the Al surface having a distorted local structure, which appeared to be the most active Ti species for hydriding catalysis of a desorbed $NaAlH_4$. At 225 °C, Ti migrated from the Al surface to the bulk, forming amorphous $TiAl_3$ clusters. This surface to bulk migration of the Ti atoms was accompanied by a deactivation of the catalyst. Subsequently, the $TiAl_3$ clusters agglomerated during the heat treatment to 475 °C to crystalline $TiAl_3$, leading to a lower dispersion of the Ti catalyst and consequently a lower hydriding activity.

Acknowledgment. This work was financially supported by ACTS, Project Number 053.61.02, and HASYLAB, Project Number I-05-062 EC. We thank Dr. P. Paulus (Shell Research and Technology Centre) for performing the XRD measurements. We also thank Dr. Konstantin Klementiev from HASYLAB for providing $TiAl_3$. Dr. Andy Beale and Prof. Dr. Diek Konings-

berger from Utrecht University are thanked for useful discussions regarding EXAFS analysis.

References and Notes

(1) Grant, P. *Nature* **2003**, *424*, 129−130.
(2) Schlapbach, L.; Züttel, A. *Nature* **2001**, *414*, 353−358.
(3) Schüth, F. *Nature* **2005**, *434*, 712−713.
(4) Wagemans, R. W .P.; Van Lenthe, J. H.; De Jongh, P. E.; Van Dillen, A. J.; De Jong, K. P. *J. Am. Chem. Soc.* **2005**, *127* (47), 16675−16680.
(5) Nijkamp, M. G.; Raaymakers, J. E. M. J.; Van Dillen, A. J.; De Jong, K. P. *Appl. Phys. A: Mater. Sci. Process.* **2001**, *72* (5), 619−623.
(6) Weitkamp, J.; Fritz, M.; Ernst, S. *Int. J. Hydrogen Energy* **1995**, *20*, 967−970.
(7) Bogdanovic, B.; Schwickardi, M. *J. Alloys Compd.* **1997**, *253*−*254*, 1−9.
(8) Baldé, C. P.; Hereijgers, B. P. C.; Bitter, J. H.; De Jong, K. P. *Angew. Chem., Int. Ed.* **2006**, *45* (21), 3501−3503.
(9) Haiduc, A. G.; Stil, H. A.; Schwarz, M. A.; Paulus, P.; Geerlings, J. J. C. *J. Alloys Compd.* **2005**, *393* (1−2), 252−263.
(10) Jensen, C. M.; Zidan, R. A.; Mariels, N.; Hee, A. G.; Hagen, C. *Int. J. Hydrogen Energy* **1999**, *24*, 461.
(11) Bellosta von Colbe, J. M.; Bogdanovic, B.; Felderhof M.; Pommerin, A.; Schuth, F. *J. Alloys Compd.* **2004**, *370*, 104−109.
(12) Bellosta Von Colbe, J. M.; Schmidt, W.; Felderhoff, M.; Bogdanovic, B.; Schüth, F. *Angew. Chem., Int. Ed.* **2006**, *45* (22), 3663−3665.
(13) Palumbo, O.; Paolone, A.; Cantelli, R.; Jensen, C. M.; Sulic, M. *J. Phys. Chem. B* **2006**, *110*, 9105−9111.
(14) Moysés Araújo, C.; Li, S.; Ahuja, R.; Jena, P. *Phys. Rev. B: Condens. Matter Mater. Phys.* **2005**, *72*, 165101.
(15) Fu, Q. J.; Ramirez-Cuesta, A. J.; Tsang, S. H. *J. Phys. Chem. B* **2006**, *110*, 711−715.
(16) Streukens, G.; Bogdanovic, B.; Felderhof, M.; Schüth, F. *Phys. Chem. Chem. Phys.* **2006**, *8*, 2889−2892.
(17) Felderhoff, M.; Klementiev, K.; Grunert, W.; Spliethoff, B.; Tesche, B.; Bellosta Von Colbe, J. M.; Bogdanovic, B.; Hartel, M.; Pommerin, A.; Schüth, F.; Weidenthaler, C. *Phys. Chem. Chem. Phys.* **2004**, *6*, 4369−4374.
(18) Bogdanovic, B.; Felderhof, M.; Germann, M.; Pommerin, A.; Schüth, F.; Weidentaler, C.; Zibrowius, B. *J. Alloys Compd.* **2003**, *350*, 246−255.
(19) Brinks, H. W.; Jensen, C. M.; Srinivasan, S. S.; Hauback, D. C.; Blanchard, D.; Murphy, K. *J. Alloys Compd.* **2004**, *376*, 215.
(20) Léon, A.; Kircher, O.; Fichtner, M.; Rothe, J.; Schild, D. *J. Phys. Chem. B* **2006**, *110*, 1192−1200.
(21) Gomes, S.; Renaudin, G.; Hagemann, H.; Yvon, K.; Sulic, M.; Jensen, C. M. *J. Alloys Compd.* **2005**, *390*, 305.
(22) Araújo, C. M.; Ahuja, R.; Guillén, J. M. O.; Jena, P. *Appl. Phys. Lett.* **2005**, *86*, 251913
(23) Iniguez, J.; Yildirim, T.; Udovic, T. J.; Sulic, M.; Jensen, C. M. *Phys. Rev. B: Condens. Matter Mater. Phys.* **2004**, *70*, 060101(R).
(24) Liu, J.; Ge, Q. *Chem. Commun.* **2006**, 1822−1824.
(25) Løvvik, O. M.; Opalka, S. M. *Appl. Phys. Lett.* **2006**, *88*, 161917.
(26) Chaudhuri, S.; Muckerman, J. T. *J. Phys. Chem. B* **2005**, *109* (15), 6952−6957.
(27) Løvvik, O. M.; Opalka, S. A. *Phys. Rev. B: Condens. Matter Mater. Phys.* **2005**, *71* (5), 054103.
(28) Graetz, J.; Reilly, J. J.; Johnson, J.; Ignatov, A. Y.; Tyson, T. A. *Appl. Phys. Lett.* **2004**, *85* (3), 500−502.
(29) Vaarkamp, M.; Linders, J. C.; Koningsberger, D. C. *Physica B* **1995**, *208/209*, 159.
(30) Teo, B. K. *EXAFS: Basic Principals and data analysis*; Springer: New York, 1986.
(31) Cook J. W., Jr.; Sayers, D. E. *J. Appl. Phys.* **1981**, *52*, 5024.
(32) Zabinsky, S. I.; Rehr, J. J.; Ankudinov, A. L.; Albers, R. C.; Eller, H. J. *Phys. Rev. B: Condens. Matter Mater. Phys.* **1995**, *52*, 2995.
(33) Koningsberger, D. C.; Mojet, B. L.; Van Dorssen, G. E.; Ramaker, D. E. *Top. Catal.* **2000**, *10* (3−4), 143−155.
(34) Li, G. G.; Bridges, F.; Booth, C. H. *Phys. Rev. B* **1995**, *52*, 6332.
(35) Norby, P.; Christensen, A. N. *Acta Chem. Scand., Ser. A* **1986**, *40*, 157−159.
(36) Klemm, W.; Krose, E. *Z. Anorg. Allg. Chem.* **1947**, *253*, 218−225.
(37) Léon, A.; Schild, D.; Fichtner, M. *J. Alloys Compd.* **2005**, *404*, 766−770.
(38) Stern, E. A. *Phys. Rev. B* **1993**, *48*, 9825.